INTERNATIONAL ATOMIC ENERGY AGENCY
UNITED NATIONS EDUCATIONAL, SCIENTIFIC AND CULTURAL ORGANIZATION

INTERNATIONAL CENTRE FOR THEORETICAL PHYSICS
34100 TRIESTE (ITALY) - P.O.B. 586 - MIRAMARE - STRADA COSTIERA 11 - TELEPHONES: 224281/2/3/4/5/6
CABLE: CENTRATOM - TELEX 460392 - I

H4.SMR/164 -17

WORKSHOP ON CLOUD PHYSICS AND CLIMATE

23 November - 20 December 1985

TROPICAL CONVECTION

(Part 2)

G. VALI
University of Wyoming
U.S.A.

LECTURE 2. TROPICAL CONVECTION

Early studies – 1950's Venezuela, Costa Rica ...
Major field experiments – 1970's AMTEX, BOMEX, GATE, MONEX
Cloud microphysics – Hawaii, FACE
Recent projects – Ivory Coast 1982-5, Hawaii 1985

Operational cloud seeding – Kenya, Thailand, Cuba, Bombay, ...

Concentrate on observations over oceans: more data; no topographical and other influences; global importance

BOUNDARY LAYER (for fair weather)

Sea surface (differs from land) – uniform, always wet, slowly changing (large heat capacity, radiation penetrates)

Mixed layer 500-800 m (vs 1 km over land) — LeMone Fig. 1
θ_v = const, q = const

Buoyancy flux decreases with altitude, slightly negative at cld. base — LeMone Fig 3

CLOUD DISTRIBUTIONS

Non-uniform. Patches from synoptic (1000 km) to small mesoscale (10-100 km). Due to variations in sea surface temperature and air mass histories.

Cloud sizes and proportions: — Warner Fig 8. J. Appl. Meteor. 1989 p. 1516
Larger clouds are more slender (only for isolated clouds)

Cu. fr. – one cloud per 1 km² — Warner & Grumm M. Wea. Rev. 1984, p 153
Cu. con. – one cloud per 1500 km²

Fraction of clouds with updrafts ~0.1 - 1%

CUMULONIMBUS

Major sources of precipitation.

Updraft and downdraft structures. — LeMone & Zipser I & II J. Atm. Sci. 1980, p2444 –

- definitions – Fig. 2
- diameter, mean and maximum magnitudes are log-normally distributed at a given altitude; updrafts are stronger than downdrafts. – Fig 3
- variations with altitude: updrafts peak at middle levels, downdrafts vary little – Fig. 1 – Fig. 4

Schematic structure

Wide, well-defined areas of updraft at cloud base, at leading edge of storm

Updrafts are narrower and stronger aloft.

Coincident with areas of precipitation there are mixtures of up and downdrafts aloft.

Wide downdraft at cloud base with precipitation – produces gust outflow.

SYSTEMS — Houze & Hobbs Adv. Geophys. Vol. 24 1982, 225-315

Squall lines

Fast motion ~15 m s⁻¹

Sharp leading edge, line or arc.

Strong cells followed by stratiform precipitation within ~100 km band

Non-squall clusters

Slow motion – few m s⁻¹

Evolution from major cells to stratiform precipitation over 2-6 hour lifetime.

Monsoon

Large-scale convergence

Stratiform with embedded convection

Hurricanes

MICROSTRUCTURE

Generally not well studied.

Coalescence and ice processes both active.

Hawaii – Takahashi warm rain obs. and models

Winter MONEX ice data — Houze and Churchill J. Atm. Sci. 1984 p.3405

CASE STUDY

GATE, DAY 261 (Sept. 18, 1974)

Observations of clouds and radar echoes

Warner & Austin 1978 M. Wea. Rev. p.983

Warner et al 1980 M. Wea. Rev. p.169

Turpeinen and Yau, 1981. M. Wea. Rev. p 1495

Models:

Turpeinen and Yau loc. cit.

Nicolini
Bader et al
Ou
Veltishchev & Polazhaev

} Modelling Workshop Jeesoe, 1985 to be published by WMO

AIR WEATHER CUMULUS OVER SEA

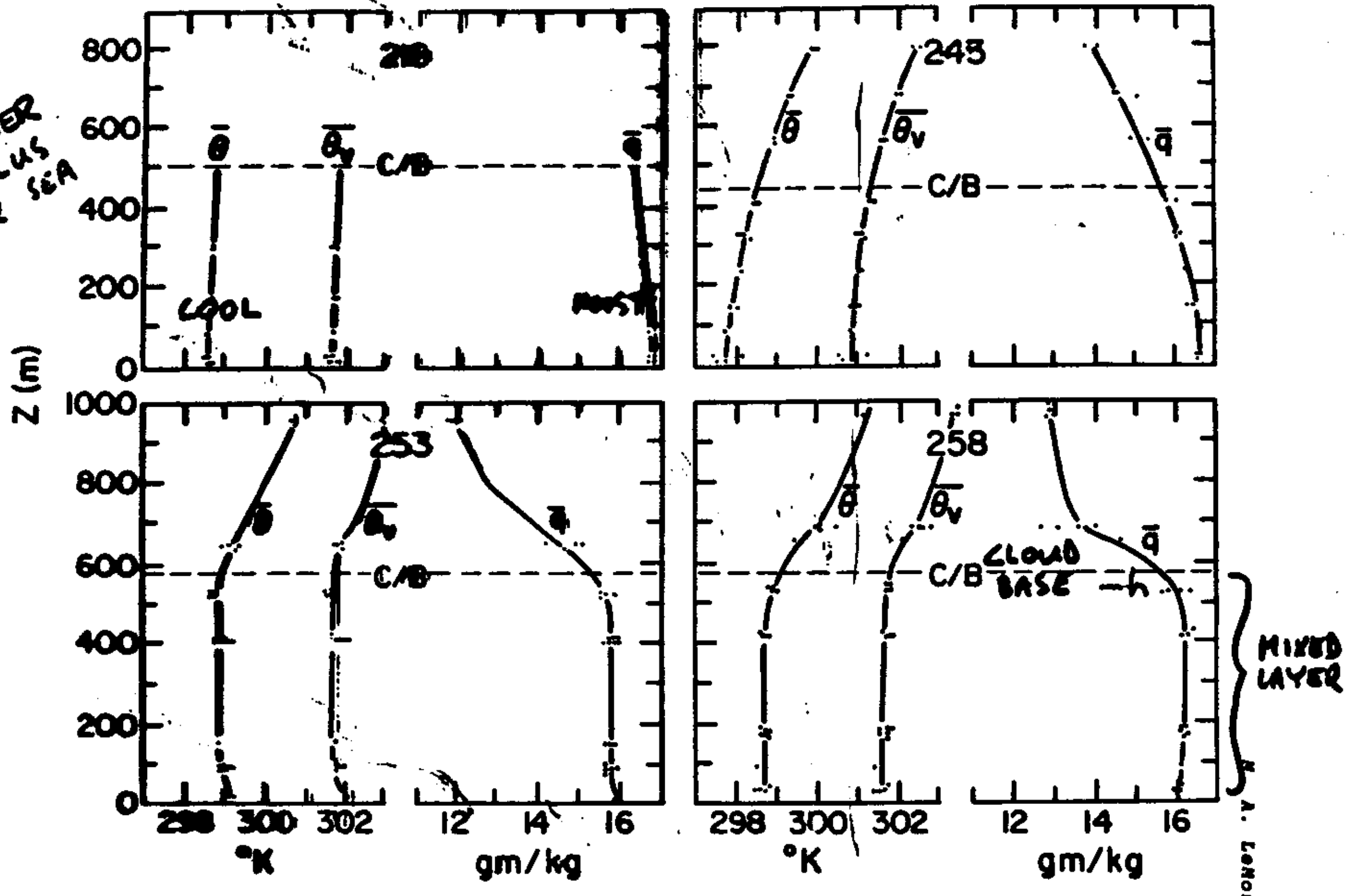

Fig. 1 Profile of potential temperature, θ; virtual potential temperature, θ_v; and specific humidity, q, for 4 days in GATE (Day 218 = 6 Aug.; Day 243 = 31 Aug.; Day 253 = 10 Sept.; Day 248 = 15 Sept., all 1974).

M. A. LeMone, 1978

2

WARNER 1981 J. Atm. Sci. p. 1816

Aircraft obs.

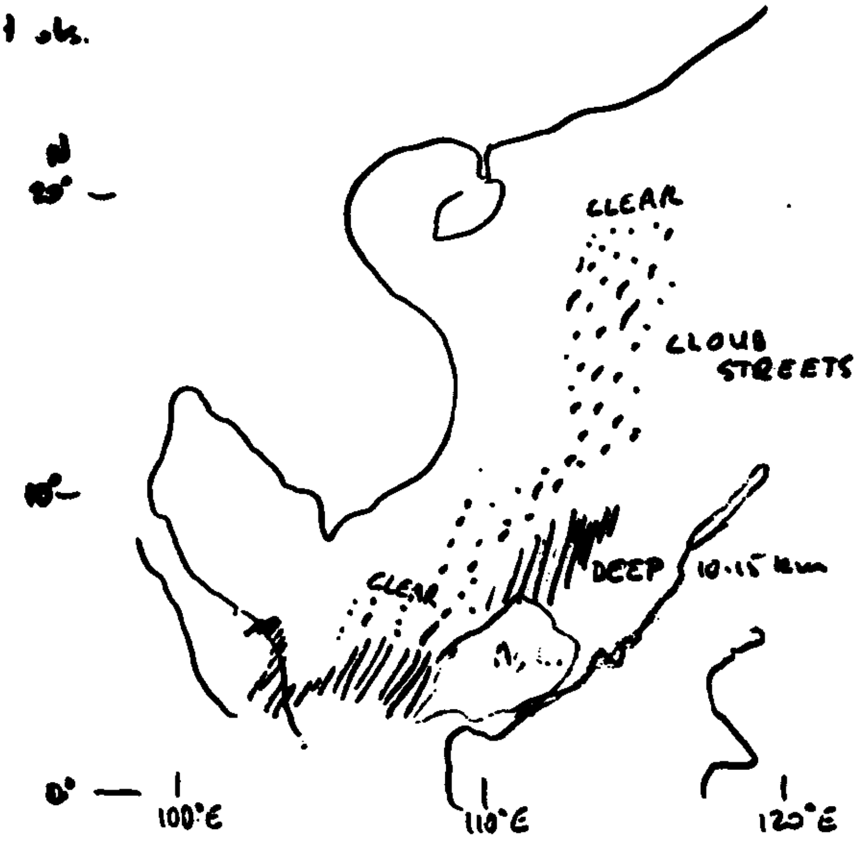

DECEMBER 10, 1978

3

WARNER, J. Appl. Meteor. 1981, p1516 4

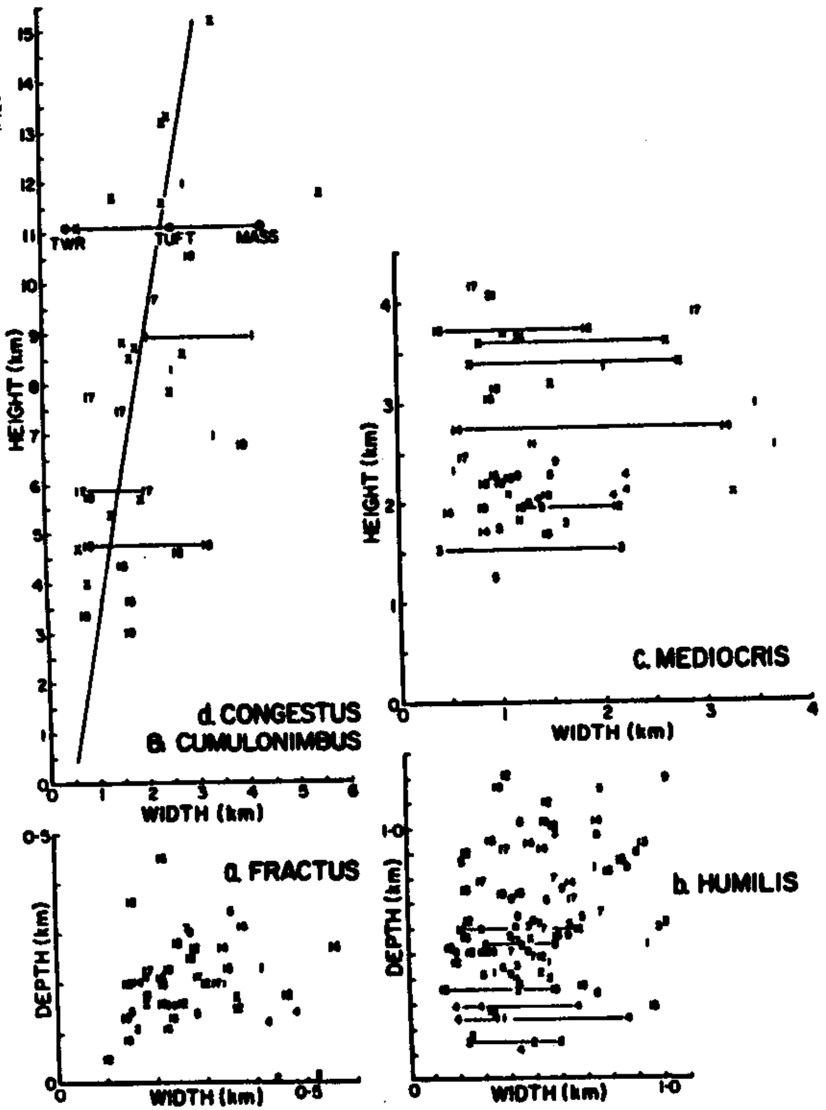

FIG. 8. 10 December 1978. Depth or height above the sea of cumulus clouds as a function of width of updraft, in the size categories *a*, fractus; *b*, humilis; *c*, mediocris, and *d*, congestus and cumulonimbus. Most measurement points are shown as small integers (1–21) referring to proximity to a corresponding dropwindsonde released from the WP3D aircraft. Pairs of measurements joined by horizontal lines show the widths of both small rising towers and the cloud masses from which the towers emerged. In *d*, a line has been drawn by eye to describe approximately the increase of width of updrafts with height.

Warner, Grumm M. Wea. Rev. 5

re, era ard ely ed wo ds ess on will

ain nd ear fig. tm

ain rs, us, p- en ed ng ld ed as us us ce in ng

ci- ns ral ed ers es- nd

les

ght ew is- r a- mt 0). ag- he

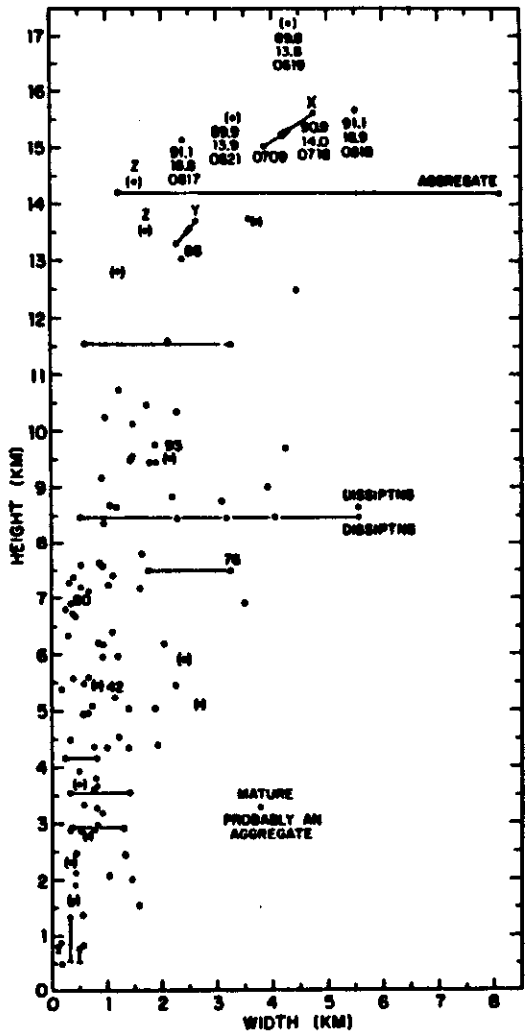

FIG. 5. Height above the sea of cumulus cloud tops as a function of width of updraft. Pairs of measurements joined by horizontal lines show the widths of both small rising towers and the cloud masses from which the towers emerged. Uncertainties are a few hundred meters for widths and range from a few hundred meters to ±2 km for heights (depending on distance from the aircraft). Points relatively uncertain in height are enclosed in parentheses. Three measurements of cloud bases are indicated by the bases of vertical bars (at bottom left). A few clouds are identified for cross-reference, the tallest with longitude (°E), latitude (°N) and GMT. Two-digit integers show rise rates of towers in tenths of meters per second.

Two points are mad appreciably from wint *et al.*, 1978; Warner, 1 1980; LeMone and 2 should be consistent w Sizes of cumulus inc (Simpson *et al.*, 1965 a cloud radius consta observations.

4. Fractional area cov

Color 35-mm slides, hPa by Warner and fr offer better resolution movies. Following the tion 2, visual assessme tional area coverage (below the 700 hPa lev 700 and 250 hPa), (d) level) and (e) the tota erages are denoted σ_R fecting vertical fluxes "by cumulus updraft where we find that σ_R

In the categories (a) shown in Fig. 6. The of each slide was plot σ were made out to a r an area of ~5000 km erage in tenths was cha to half the maximum there was obscuration over ranges less than small area of view), th theses in Fig. 6. The an assessment was im by cloud in a differen are incomplete in cov

Coverage σ_R by cun cloud line near 92°E, low infrared brightnes was small. In the nort Coverage by low strat with small-scale variat

Mid-level stratus (F cloud type with respe classification MF in Fi masses of high clouds the north Bay, althoug The TIROS-N infrared *al.*, 1980) does not indi mid-level stratus layers

6

Warner & Gamm
1984, M. Wea. Rev.
p 153

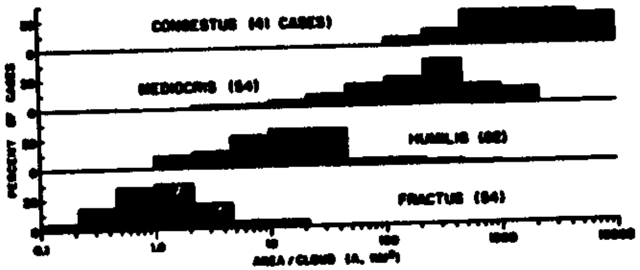

FIG. 7. Histograms of inverse cloud number densities, or horizontal areas per cloud, in the categories fractus, humilis, mediocris and congestus. The uncertainty is nominally a factor of 2.

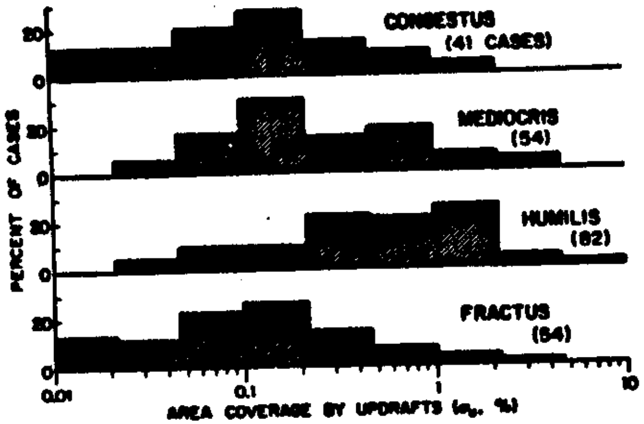

FIG. 8. Histograms of percent area coverage by updrafts σ_u. Categories as in Fig. 7. The uncertainty is nominally a factor of 10.

Warner & Gamm, 1984
M. Wea. Rev. p.153

TABLE 3. Median values of inverse cloud number densities, area coverages by updrafts and area mean ascent rates for different size categories of cumulus.

Cumulus category	Fractus	Humilis	Mediocris	Congestus
Approximate height of assessments (km)	0.7	1	2	4
Median area of assessments (km^2)	18	120	770	3000
Median A (km^2 $cloud^{-1}$) (Fig. 7)	1.1	14	220	1500
Median width of cloud updraft (m)	40	300	800	1500
Median σ_u (%) (Fig. 8)	0.10	0.54	0.20	0.11
Stipulated mean updraft speed (m s^{-1})	small	1.0	2.5	2.5
Median $\bar{\omega}$ (Pa s^{-1}) (Fig. 9)	small	−0.06	−0.05	−0.02

FRACTION OF CLOUD WITH UPDRAFT

AREA MEAN ASCENT

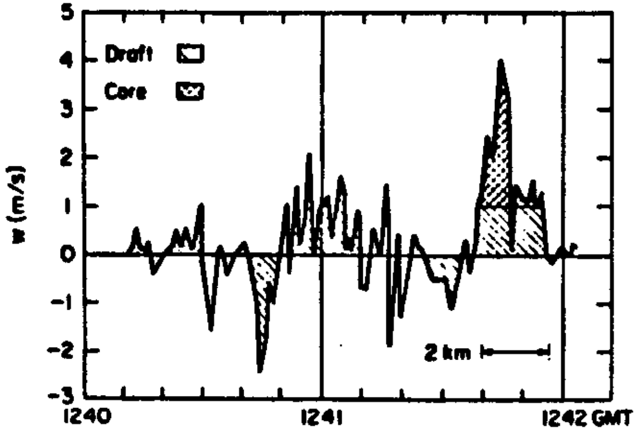

FIG. 2. Time series illustrating definition of drafts and cores, adapted from US C-130 at 5471 m. Day 257. An updraft has to reach 0.5 m s^{-1} and be positive for 0.5 km (~5 s) or more; a core has to have w of at least 1 m s^{-1} for 0.5 km or more. Downdrafts and downdraft cores are defined in the same way. Note that the draft at the right has two cores.

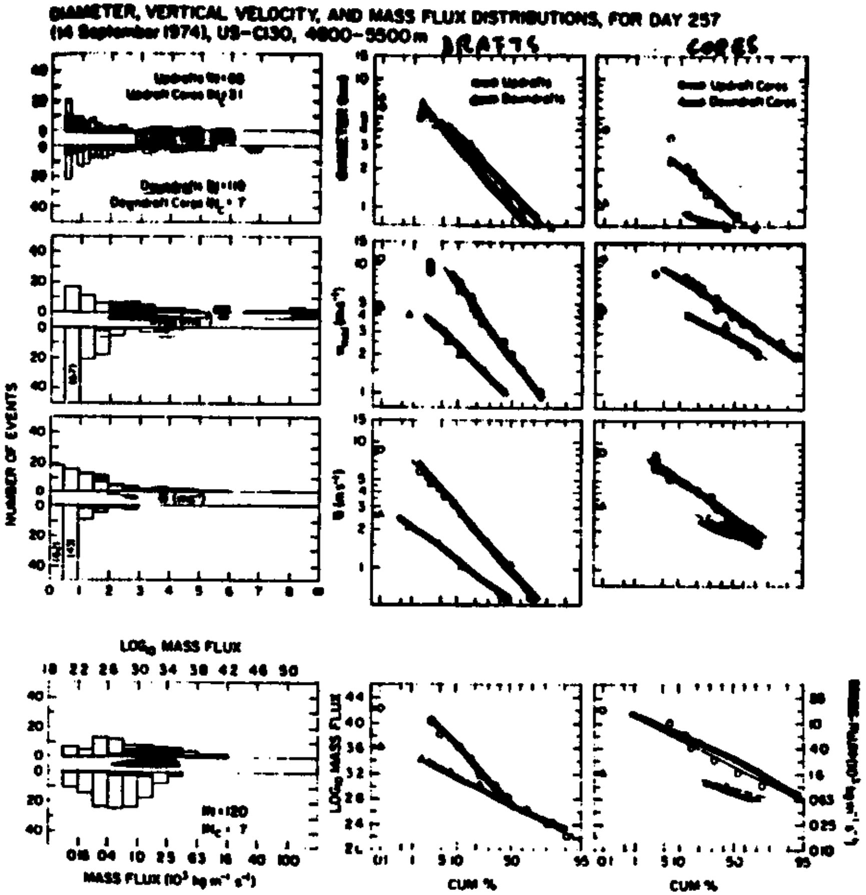

FIG. 3. Diameter, vertical velocity and mass flux distributions for Day 257 (14 September 1974), at 4800–5500 m, from the US C-130. In the left column of the figure, the upward extending bars of the graph are for updrafts, the downward extending bars are for downdrafts. For updraft: (1) bars: total length is total number of drafts; black is number of cores; (2) bars: total length is total number of cores; clear, number of drafts. Downdrafts and downdraft cores are coded analogously. Cumulative distributions for drafts are in the middle column; cumulative distributions for cores are in the right column.

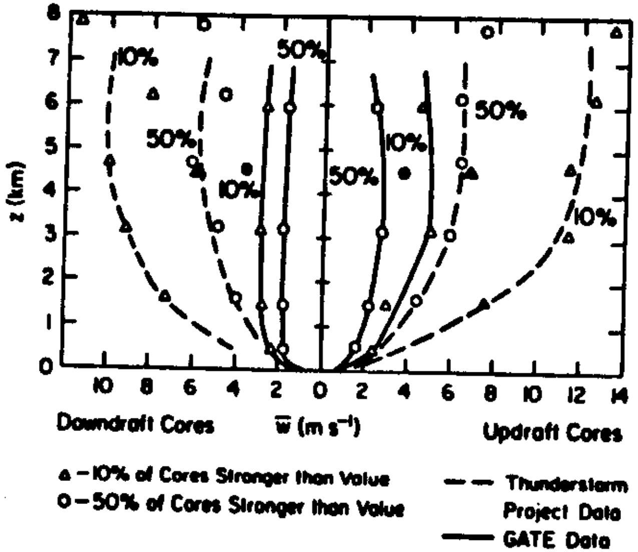

FIG. 1. Mean vertical velocity in updraft and downdraft cores as a function of height, comparing different data sets. The GATE data for strong (10% level) and median (50% level) cores are taken from Fig. 5 of LZ. The Thunderstorm Project Data defined in the same way are adopted from Byers and Braham (1949), Tables 7 and 10. For the 4.5 km level only, data from Gray (1965), Fig. 13, defined similarly, are included (filled symbols).

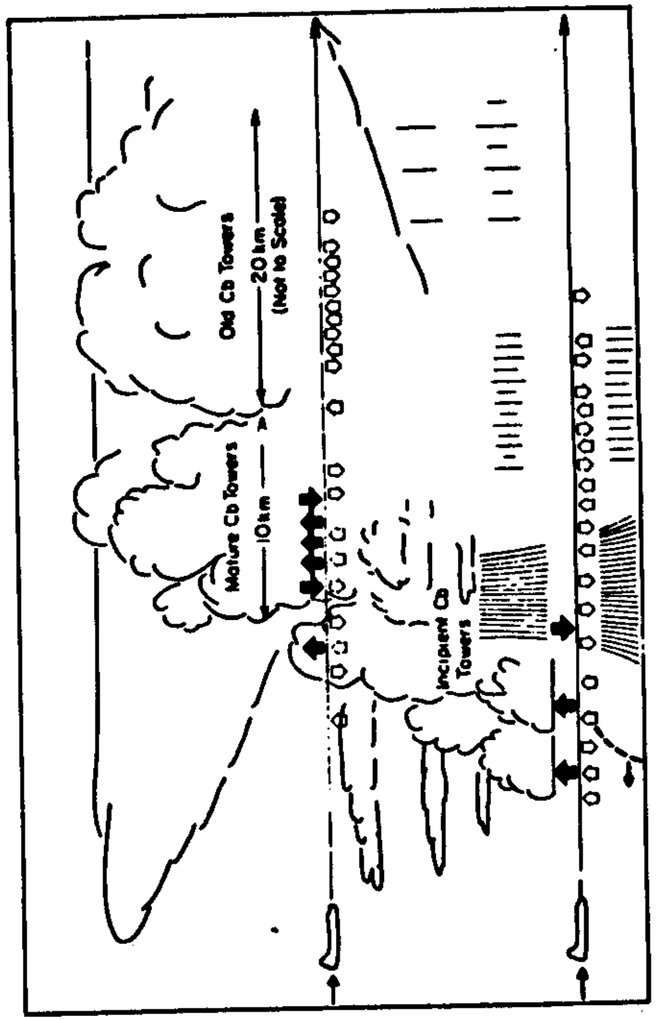

FIG. 4. Schematic of "typical" aircraft passes through a convective band, showing location of drafts and cores near cloud base and in the middle troposphere. There are wide variations from day to day and from one pass to the next on any given day. An average leg is 90 km in length, half of which would be involved with clouds and precipitation and which would contain most of the drafts and cores.

Houze and Churchill 1984

12

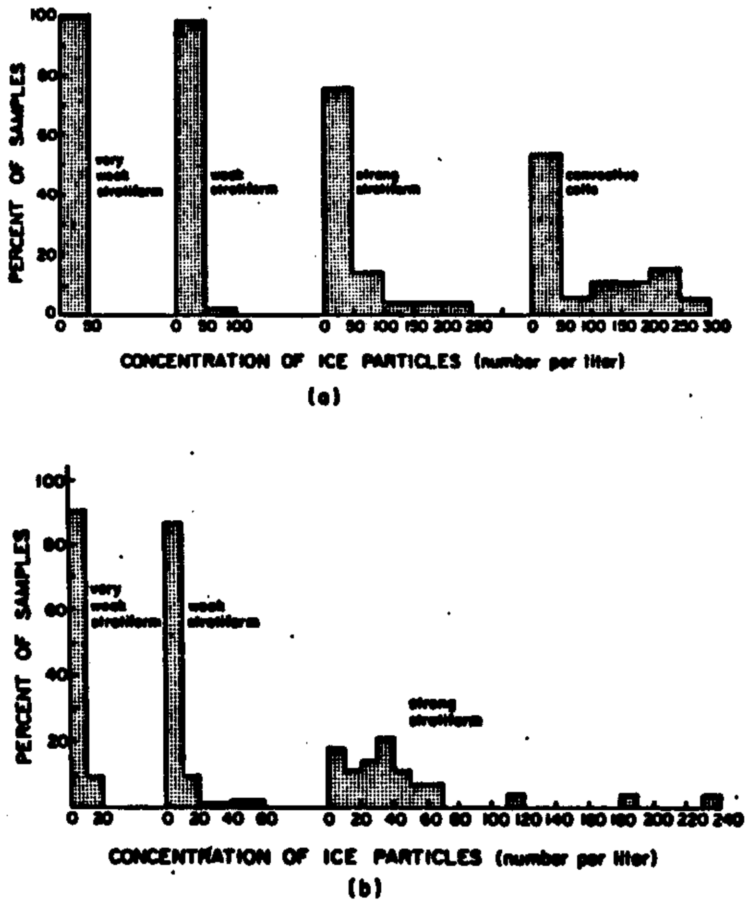

FIG. 1. Concentrations of particles observed with the PMS cloud probe (upper particle size limit 1.6 mm) aboard the NOAA WP-3D aircraft during Winter MONEX. Observations were made at altitudes of 7–8 km (−14 to −19°C) and the concentrations referred to were 1 min averages. The categories very weak stratiform, weak stratiform, strong stratiform and convective cells describe the precipitation through which the aircraft was flying. In (a) an increment of 50 per liter on the abscissa was used in plotting the histograms. In (b) an increment of 10 per liter was used to show more detail in the stratiform categories.

contradict this expectation. The absence of pristine crystal shapes suggests either that growth by vapor deposition was not effective or the crystals were too small to be identified.

There are several possible explanations for the observed high concentrations of small hydrometeors

regions penetrated by the P3 were associated with strong updrafts and downdrafts (vertical velocities greater than 2 m s^{-1}). The high concentrations of small particles in these regions could be explained either by ice being generated at low levels and lifted to flight level by convective updrafts or by nucleation

13

M. Wea. Rev. 1981, p 1495

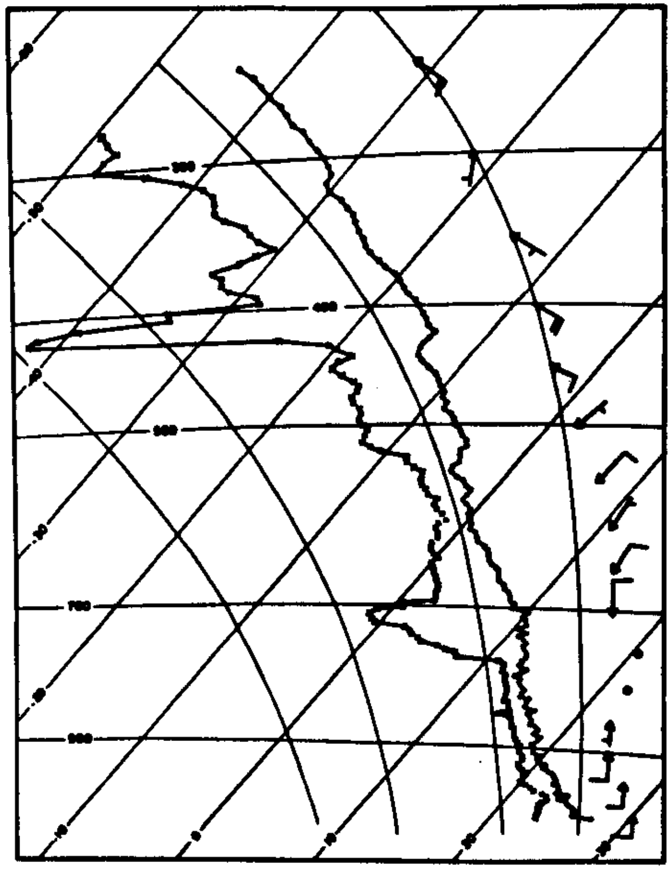

FIG. 1. Sounding made at 1200 GMT plotted on a tephigram.

…hal angles from 357–5° also was …ntenna was moving from one el…t in that interval.

…a vertical resolution of 5 mb made …a at 0600, 1200 and 1500 GMT on …ained from the Atmospheric En-

The synoptic situation on this day is characterized by the approach and passage of a ridge axis of an easterly wave at 700 mb over the center of the GATE A/B-scale network (Thompson *et al.*, 1979). The temperature and dew-point profiles indicate undisturbed conditions as objectively classified by

GATE
261
SATELLITE
ANAL
1352 GMT

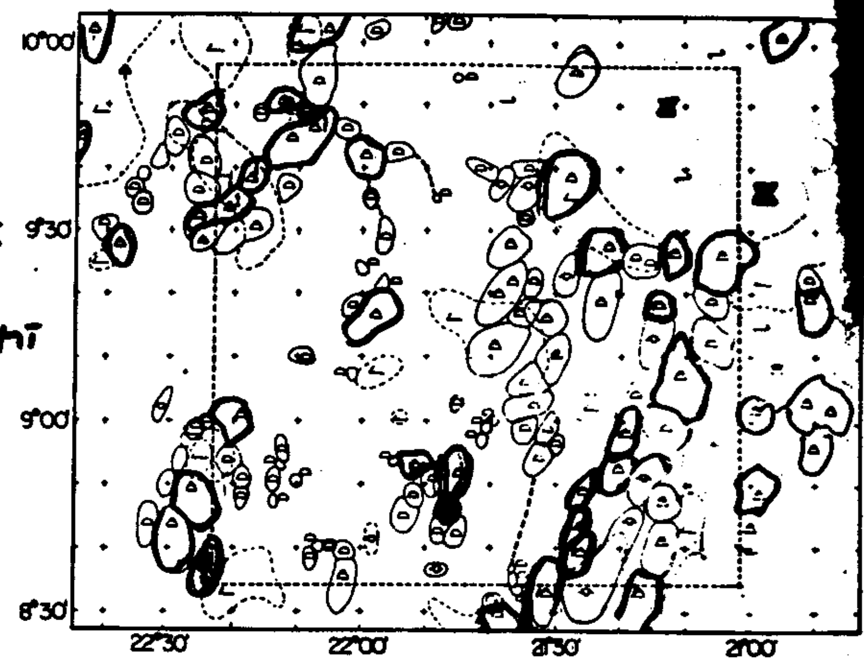

FIG. 1. 1352 GMT. Cloud coverage from a map of digital cloud-brightness in the visible channel of SMS-1. All clouds resolved in the contoured digital data, of resolution ~2 km, are represented. Solid lines show cumulus (including cumulonimbus), dashed lines show stratiform and dotted lines show cirriform clouds. Heavy dashed lines mark lines of very small cumulus. Divisions between adjacent clouds are based on brightness gradients. Cloud types were determined by viewing sequences of full resolution visible and infrared images centered on 1352 GMT. The box marks the [illegible] of the aircraft.

14

FIG. 10. Wall chart of radar B-scans. Time (GMT) along abscissa. [illegible]

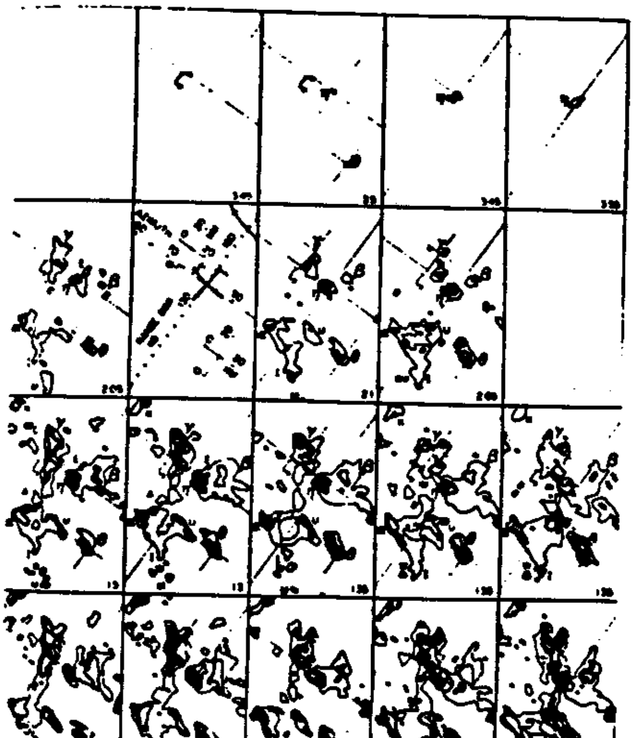

FIG. 10 (Continued)

15

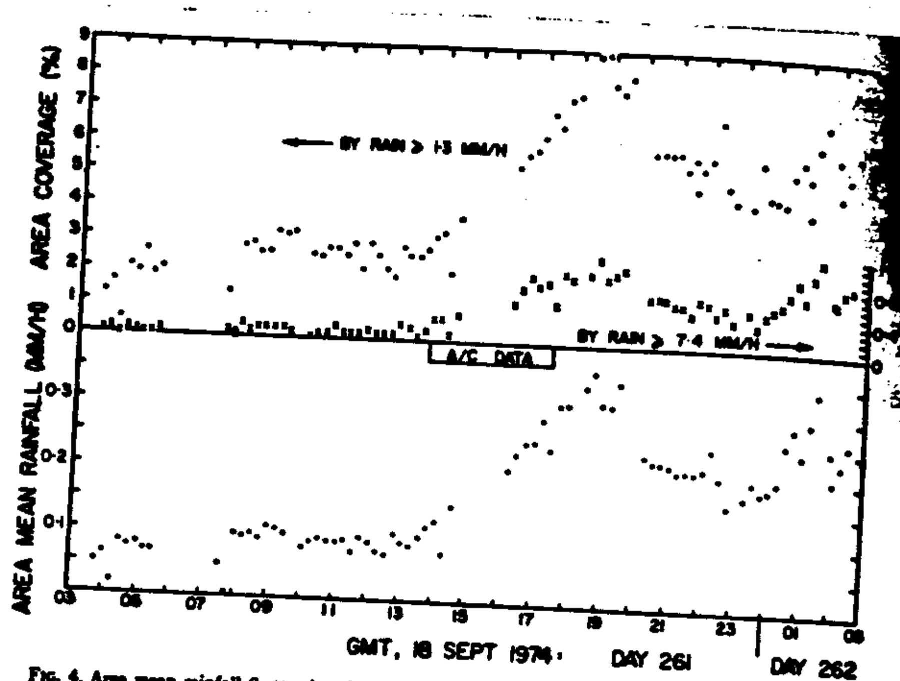

FIG. 4. Area mean rainfall (bottom) and percent area coverage (top) by reflectivities exceeding each of the two thresholds 24 and 36.5 dBZ, as a function of time. (From Table 2, 24 and 35.5 dBZ are equivalent to 1.3 and 7.4 mm h^{-1}.) The area of the radar field of view was 138 000 km^2. The data are from measurement "bins" of area 17.6 km^2. The time interval of aircraft data collection is shown. Isolated irregularities probably are artificial, due to ship motion.

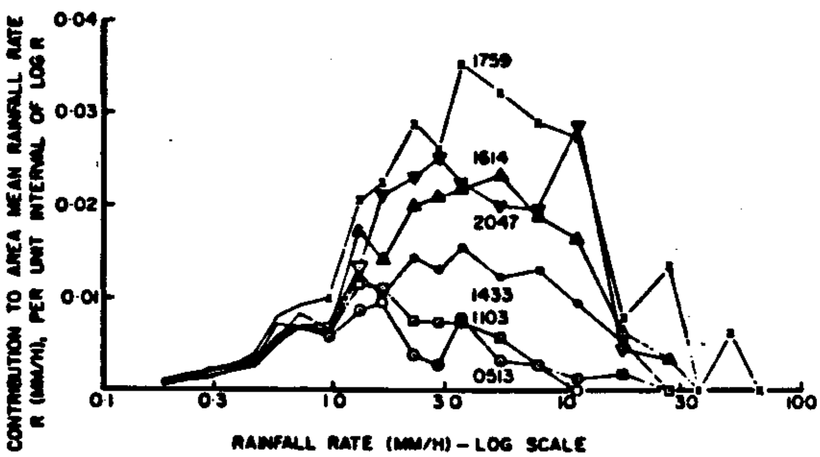

FIG. 6. Distribution with rate of rainfall over radar field of view showing counts of bins with rain multiplied by rate, plotted against rate on a log scale. For different times as indicated. (The curves should be in stepped at thresholds, as usual for a histogram; points are joined instead, for clarity.)

18

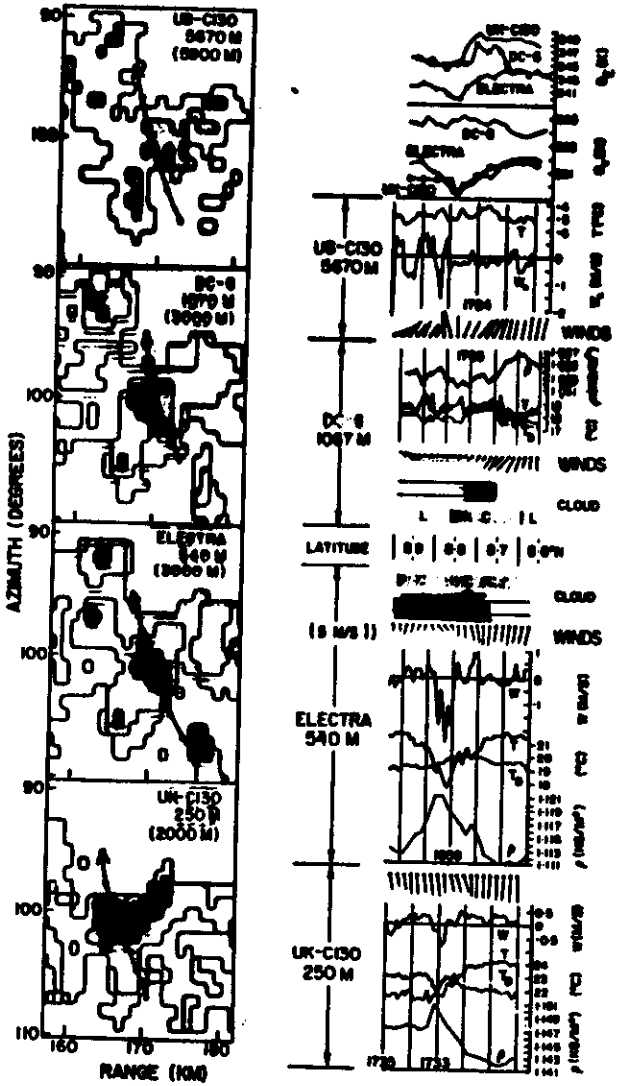

Fig. 15 (Left). Tracks of four aircraft through radar echo group P. Dots are at minute intervals, comparable with Fig. 16. Flight altitude is shown, and approximate altitude of radar scan is in parentheses. Maps are elements of B-scans with coordinates of azimuth and range from the *Quadra* radar. For the location of group P see Fig. 11 (bottom right). Reflectivity contours at 23, 27, 34 and 44 dBZ. Profiles of reflectivity shown in Fig. 13e.

Fig. 16. (Right). Time-series plots of data from four aircraft, penetrating echo group P (Fig 15). The plots are keyed to geographical location, shown in the middle. See text for details. Winds are represented by barbs: a wind of 5 m s^{-1} from 180° is as shown in parentheses at middle left. Under CLOUD, the letters C and L mean flight environments of cumulus clouds and clear air, respectively. Dense shading indicates flight within dense cloud; bars without shading indicate flight within tenuous cloud. Such observations are not given for the C130s.

19

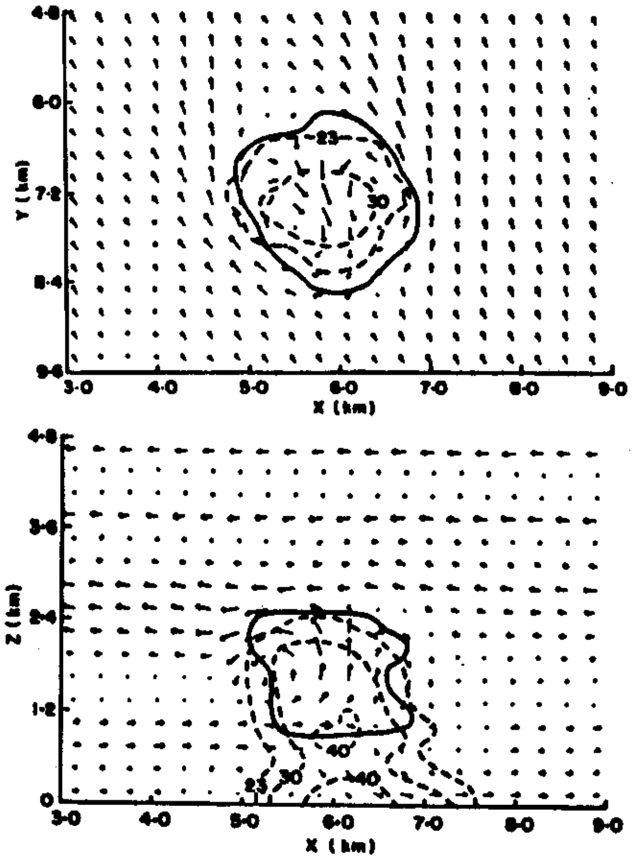

Fig. 9. Horizontal cross section of the vector velocity, cloud-water content and radar reflectivity factor at 1950 m (top) and corresponding section of the vertical plane containing the maximum updraft at $y = 7.8$ km (bottom). The solid lines indicate cloud boundaries (liquid water content ≥ 0.01 g kg^{-1}). The dashed lines are contours of radar reflectivity factor (dBZ). The arrows are vector velocities normalized by the maximum velocity at each section. Note the orientation of the axes (north at the bottom and east to the right).

Nicolini 1985 Issee Conf. 20

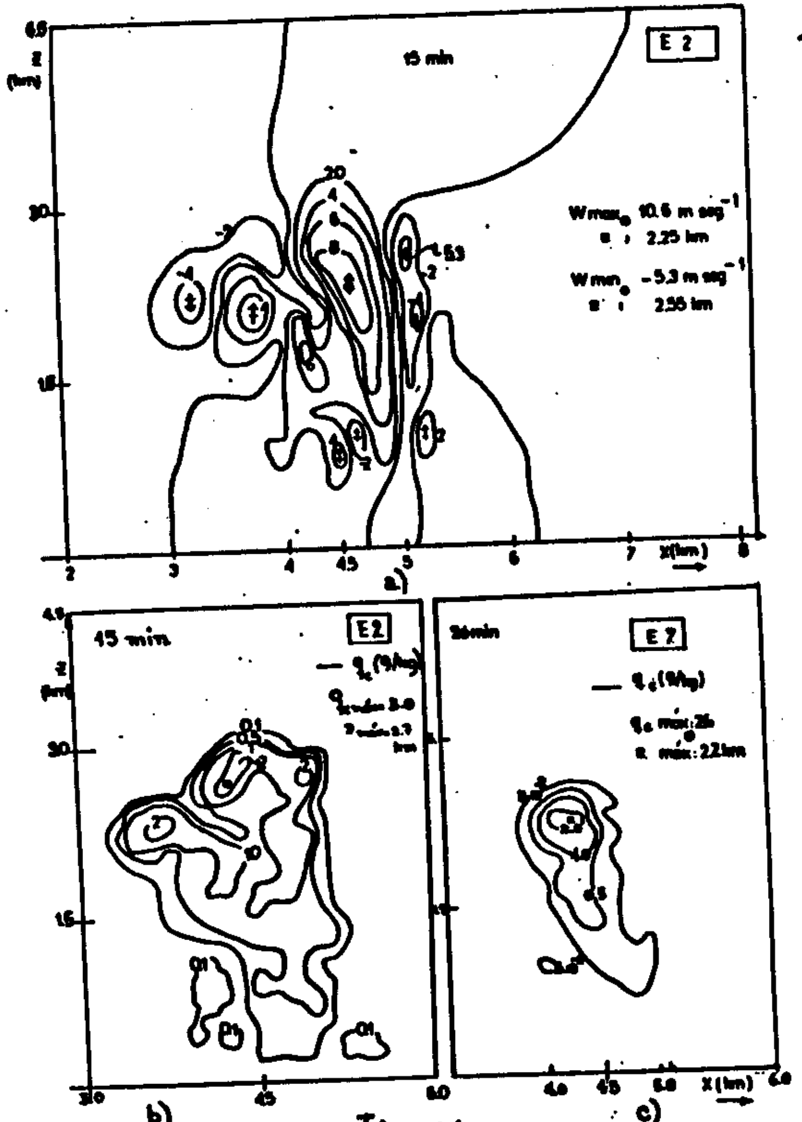

Figure 1

Figure 1: Vertical section at 15 min of the fields of: a)Vertical velocity (w)and b) cloud water mixing ratio (g/ kg), in experiment E2., c) cloud water mixing ratio (gr/kg) in experiment E7.

Issee Conf.

FIGURE 2

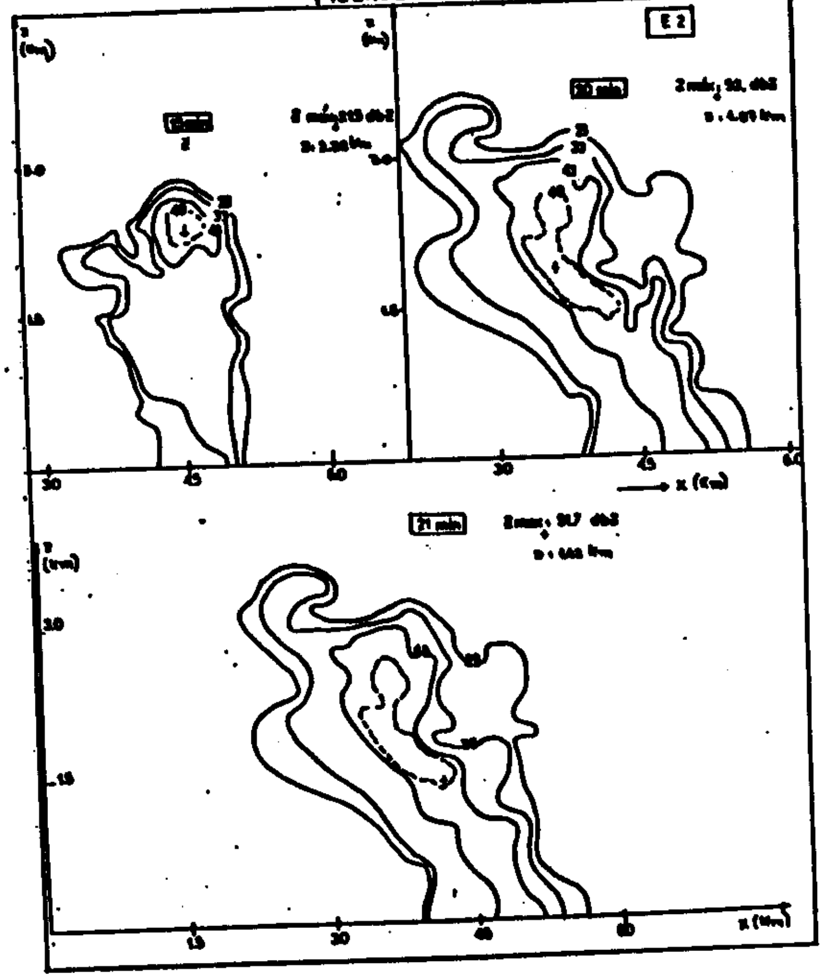

Figure II: Vertical sections at : a) 15 min, b) 20 min., and c) 21 min, of radar reflectivity factor (Z) in experiment E2.

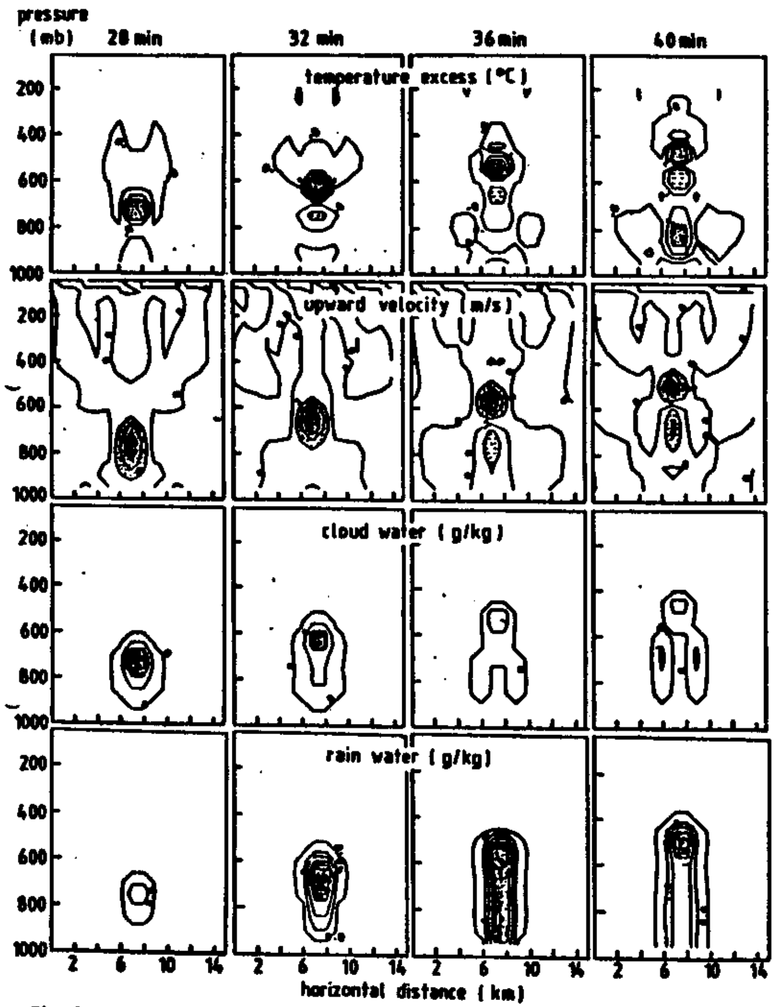

Fig. 2. Evolution of simulated GATE warm cloud. (no shear run)
Contour intervals; shaded values are:-

temperature excess	1°C;	>4°C, >2°C, <-1°C
upward velocity	2m/s;	>6m/s, >2m/s, <-2m/s
cloud water	1g/kg;	>2g/kg
rain water	0.5g/kg;	>1.5g/kg

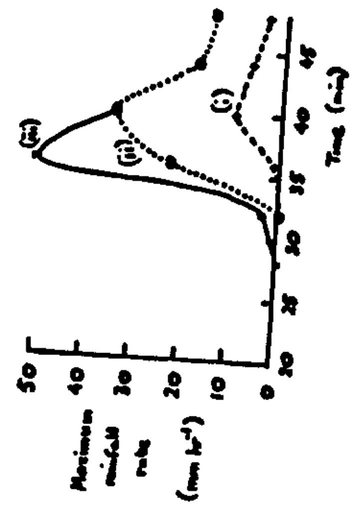

Fig. 3. Rainfall rates at the base of the model grid using the same values of α, β and l_{crit} as the model run but with γ (s^{-1}) of

(i) 0.001
(ii) 0.003 (control)
(iii) 0.005

Table 1

Comparisons of computed and observed parameters, GATE-261

Source	Height of maximum reflectivity (km)	Maximum reflectivity (dBZ)	Cell's life cycle (min)	W max in updraft (m/s)	W min in downdraft (m/s)	Maximum cloud water content (g/kg)
Mean values for isolated cells from radar observations (Table 2 in /16/)	2.4	31	28	-	-	-
Values from numerical experiment N 1 (Tables 3 and 4 in /16/)	2.4	43	22	5.2	-2.8	1.9
Values in present computations	2.1	47	21	4.6	-1.4	2.6

24

MODEL - OBSERVATION INTERCOMPARISON

Case: Gate 261

Undisturbed conditions with small-moderate cumulus.
Deeper clouds later in day.

PARAMETER	OBSERVATION	Turpeinen 3d) MODEL	(Nicolini 2d)	(Ou 1d)
CLOUD TOP	3 km	3.3 km	3 km	2.1 - 7km
CLOUD LIFETIME	20-60 min	35 min	30 min	28-60 min (to reach top)
CLOUD DIMENSION	4 km (typic.) 10 km (some)	5 km	1.5 km	
UPDRAFT MAGNITUDE	2 ms^{-1} (cloud base)	5.7 ms^{-1} at 2.1km	5.9 ms^{-1} at 2.0 km	
DOWNDRAFT MAGNITUDE		3.4 ms^{-1} at 3.0 km	4.6 ms^{-1} at 2.4 km	
CLOUD WATER	1.6 g/m^{-3} (max) at 1.1 km	2.4 g/m^{-3} (max) at 2.25 km	3.2 g/m^{-3} (max) at 2.5 km	
PRECIP AT GROUND	2 mm hr^{-1} (typ) 20 mm hr^{-1} (max)	36 mm hr^{-1} (max)	9 mm hr^{-1} (max)	2-23 mm hr^{-1}
RADAR ECHO	45 dbz (max)	48 dbz (max)	42 dbz (max)	
CLOUD MOVEMENT	variable	N wards with 900 mb wind	N wards very slow	

1d SIMULATION SENSITIVE TO MIXING AND INITIAL RADIUS

25